

Numerical Optimization of Single-chamber Mufflers Using Neural Networks and Genetic Algorithm

Ying-Chun CHANG

Department of Mechanical Engineering, Tatung University-TAIWAN R.O.C.

Min-Chie CHIU

Department of Automatic Control Engineering, Chungchou Institute of Technology- TAIWAN R.O.C.

e-mail: minchie.chiu@msa.hinet.net

Received 04.06.2008

Abstract

To simplify the optimization process, a simplified mathematical model of a muffler is constructed using a neural network and a series of input design data (muffler dimensions) and output data (theoretical sound transmission loss) that are obtained by utilizing a theoretical mathematical model (TMM). To assess an optimal muffler, a neural network model (NNM) is used as the objective function in conjunction with a genetic algorithm (GA). Before the GA operation can be carried out, however, the accuracy of the TMM must be checked and be in accord with the experimental data. Additionally, the NNM must also be in agreement with the TMM. Also discussed are the numerical cases of sound elimination relative to the various parameter sets and pure tones (500, 1000, and 2000 Hz). The results reveal that the maximum value of the sound transmission loss (STL) can be accurately obtained at the desired frequencies. Consequently, the algorithm proposed in this study can provide an efficient way to develop optimal silencers for the requisite industries.

Key Words: Four-pole transfer matrix, Polynomial neural network model, Optimization, Genetic algorithm.

Introduction

High noise levels can actually cause physical harm leading to both psychological and physiological symptoms (Alley et al., 1989); therefore, the need to lower the noise level of certain pieces of machinery would seem to be of paramount concern (Kaiser and Bernhardt, 1989). In order to depress low frequency noise emitted from a venting system, a reactive muffler is customarily used (Magrab, 1975). Research on engine noise mufflers was started by Davis et al. (1954). Four-pole matrices for evaluating acoustical performances were developed by Igarashi (1958, 1959, 1960) and Miwa (1959). Studies of simple expansion mufflers based on the flow rate and temperature gradient using a pure plane wave theory have been amply addressed (Munjaj, 1987; Prasad, 1989; Kim et al., 1990).

Because of the constrained problem, which is

mostly concerned with the necessity of operation and maintenance in practical engineering work, there has been a growing need to optimize acoustical performance within a limited space. Yet, the need to investigate an optimal muffler design under space constraints is rarely tackled. In previous work (Chang et al., 2004), the shape optimizations of space-constrained straight simple-expansion mufflers using 3 kinds of gradient methods were discussed. In order to efficiently search for the optimal shape of a one-chamber muffler, a genetic algorithm (GA) has been adopted (Chang et al., 2005).

Because design parameters can easily be changed without a total overhaul of the muffler design when a polynomial neural network is used instead of the full model, a surrogate model – a trained neural network model (NNM) with a series of real data – is established and used as the new objective (OBJ) function. As the real data are very close to the theoretical data,

and to facilitate the assessment of the real data fitted to a NNM, the theoretical data are employed as the real data. In this paper, the methodology of 4-pole transfer matrices in conjunction with the NNM and the GA to maximize the STL by adjusting the muffler's shape under space constraints are exemplified and confirmed.

Theoretical Mathematical Model (TMM)

As indicated in Figure 1, the muffler system comprised of 3 elements is represented by 6 points in the

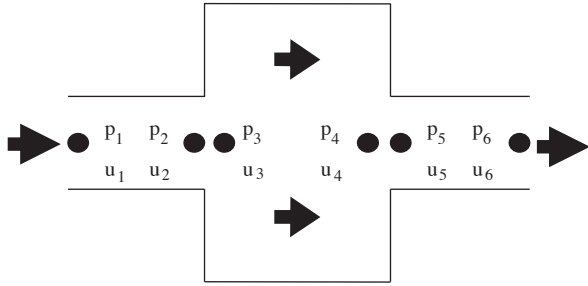


Figure 1. The acoustical nodes inside the acoustical field.

acoustical field. The related dimensions of a muffler are illustrated in Figure 2. Individual transfer matrices with respect to each case of straight ducts and expanded/contracted ducts are described (Chang et al., 2004)

As indicated in Figure 1, on the basis of the plane wave theory, the 4-pole matrix between pt 1 and 2 for a straight duct with mean flow is

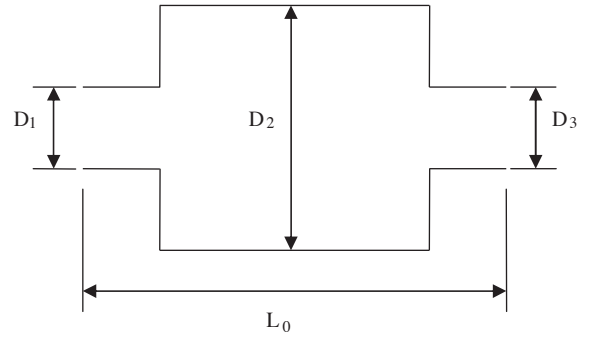


Figure 2. The outline of a one-chamber perforated muffler in a one-chamber perforated muffler.

$$\begin{pmatrix} p_1 \\ \rho_o c_o u_1 \end{pmatrix} = e^{-jM_1 k L_1 / (1-M_1^2)} \begin{bmatrix} TS1_{1,1} & TS1_{1,2} \\ TS1_{2,1} & TS1_{2,2} \end{bmatrix} \begin{pmatrix} p_2 \\ \rho_o c_o u_2 \end{pmatrix} \quad (1a)$$

where

$$TS1_{1,1} = \cos \left[\frac{kL_1}{1-M_1^2} \right]; TS1_{1,2} = j \sin \left[\frac{kL_1}{1-M_1^2} \right]; TS1_{2,1} = j \sin \left[\frac{kL_1}{1-M_1^2} \right]; TS1_{2,2} = \cos \left[\frac{kL_1}{1-M_1^2} \right] \quad (1b)$$

Similarly, the 4-pole matrix between pt 2 and 3 for a sudden expansion duct is

$$\begin{pmatrix} p_2 \\ \rho_o c_o u_2 \end{pmatrix} = \begin{bmatrix} TE1_{1,1} & TE1_{1,2} \\ TE1_{2,1} & TE1_{2,2} \end{bmatrix} \begin{pmatrix} p_3 \\ \rho_o c_o u_3 \end{pmatrix} \quad (2a)$$

$$TE1_{1,1} = 1; TE1_{1,2} = 0; TE1_{2,1} = 0; TE1_{2,2} = \frac{S_3}{S_2} \quad (2b)$$

As the derivation in Eq. (1), the 4-pole matrix between node 3 and 4 with mean flow is expressed in Eq. (3).

$$\begin{pmatrix} p_3 \\ \rho_o c_o u_3 \end{pmatrix} = e^{-jM_3 k L_2 / (1-M_3^2)} \begin{bmatrix} TS2_{1,1} & TS2_{1,2} \\ TS2_{2,1} & TS2_{2,2} \end{bmatrix} \begin{pmatrix} p_4 \\ \rho_o c_o u_4 \end{pmatrix} \quad (3a)$$

where

$$TS2_{1,1} = \cos \left[\frac{kL_2}{1-M_3^2} \right]; TS2_{1,2} = j \sin \left[\frac{kL_2}{1-M_3^2} \right]; TS2_{2,1} = j \sin \left[\frac{kL_2}{1-M_3^2} \right]; TS2_{2,2} = \cos \left[\frac{kL_2}{1-M_3^2} \right] \quad (3b)$$

Similarly, the 4-pole matrix between pt 4 and 5 for a sudden contraction duct is

$$\begin{pmatrix} p_4 \\ \rho_o c_o u_4 \end{pmatrix} = \begin{bmatrix} TE2_{1,1} & TE2_{1,2} \\ TE2_{2,1} & TE2_{2,2} \end{bmatrix} \begin{pmatrix} p_5 \\ \rho_o c_o u_5 \end{pmatrix} \quad (4a)$$

$$TE2_{1,1} = 1; TE2_{1,2} = 0; TE2_{2,1} = 0; TE2_{2,2} = \frac{S_5}{S_4} \quad (4b)$$

As the derivation in Eq. (1), the 4-pole matrix between node 5 and 6 with a mean flow is expressed in Eq. (5).

$$\begin{pmatrix} p_5 \\ \rho_o c_o u_5 \end{pmatrix} = e^{-jM_5 k L_3 / (1 - M_5^2)} \begin{bmatrix} TS3_{1,1} & TS3_{1,2} \\ TS3_{2,1} & TS3_{2,2} \end{bmatrix} \begin{pmatrix} p_6 \\ \rho_o c_o u_6 \end{pmatrix} \quad (5a)$$

where

$$TS3_{1,1} = \cos \left[\frac{kL_3}{1 - M_5^2} \right]; TS3_{1,2} = j \sin \left[\frac{kL_3}{1 - M_5^2} \right]; TS3_{2,1} = j \sin \left[\frac{kL_3}{1 - M_5^2} \right]; TS3_{2,2} = \cos \left[\frac{kL_3}{1 - M_5^2} \right] \quad (5b)$$

By a substitution and a rearrangement in Eqs. (1)-(5), the resultant system matrix of the muffler can be reduced to

$$\begin{pmatrix} p_1 \\ \rho_o c_o u_1 \end{pmatrix} = e^{-jk \left[\frac{M_1 L_1}{1 - M_1^2} + \frac{M_3 L_2}{1 - M_3^2} + \frac{M_5 L_3}{1 - M_5^2} \right]} \begin{bmatrix} TS1_{1,1} & TS1_{1,2} \\ TS1_{2,1} & TS1_{2,2} \end{bmatrix} \begin{bmatrix} TE1_{1,1} & TE1_{1,2} \\ TE1_{2,1} & TE1_{2,2} \end{bmatrix} \begin{bmatrix} TS2_{1,1} & TS2_{1,2} \\ TS2_{2,1} & TS2_{2,2} \end{bmatrix} \begin{bmatrix} TE2_{1,1} & TE2_{1,2} \\ TE2_{2,1} & TE2_{2,2} \end{bmatrix} \begin{bmatrix} TS3_{1,1} & TS3_{1,2} \\ TS3_{2,1} & TS3_{2,2} \end{bmatrix} \begin{pmatrix} p_6 \\ \rho_o c_o u_6 \end{pmatrix} \quad (6)$$

Equation (6) can subsequently be expressed as

$$\begin{pmatrix} p_1 \\ \rho_o c_o u_1 \end{pmatrix} = \begin{bmatrix} T_{11}^* & T_{12}^* \\ T_{21}^* & T_{22}^* \end{bmatrix} \begin{pmatrix} p_6 \\ \rho_o c_o u_6 \end{pmatrix} \quad (7)$$

The sound transmission loss (STL) of a muffler is defined as (Munjal, 1987)

$$STL(Q, f, L_1, L_2, L_3, D_1, D_2, D_3) = 20 \log \left(\frac{|T_{11}^* + T_{12}^* + T_{21}^* + T_{22}^*|}{2} \right) + 10 \log \left(\frac{S_1}{S_5} \right) \quad (8a)$$

$$\text{where } L_o = L_1 + L_2 + L_3 \quad (8b)$$

Neural Network Model (NNM)

The neural network used in optimization has been widely applied in various fields. It has been found that the neural network provides a great benefit in establishing an NNM by imitating a given model. In this paper, a well-known polynomial neural network will be adopted and discussed.

Concept of the polynomial neural network

Artificial neural networks (ANNs) have been successfully applied in many fields to model complex nonlinear relationships. ANNs may be viewed as the universal approximators, but the main disadvantage of this approach is that detected dependencies are hidden within the neural network structure. Conversely, when working on a better prediction of fish populations in rivers, a polynomial neural network called Group Method of Data Handling (GMDH) was developed by Ivakhnenko (1971). Ivakhnenko

made the neuron a more complex unit featuring a polynomial transfer function. The interconnections between the layers of neurons were simplified, and an automatic algorithm for structure design and weight adjustment was developed. The main idea of GMDH is to use feed-forward networks based on short-term polynomial transfer functions whose coefficients are obtained using a regression technique. The regression technique is then combined with the emulation of the self-organizing activity for the neural network (NN) structural learning. The GMDH algorithm, one kind of recognition method in a nonlinear system that can be self-organized, can establish an adaptive model, a monitoring model, and a learning model. By monitoring learning at input and output, the output data are therefore modeled by the input function implicitly.

The self-organizing adaptive model NNM is organized as follows (Kondo, 1988):

- A. Divide the original data into 2 groups - a train-

ing data group and a testing data group.

The training data group is used for evaluating the weights of the neural network. In addition, the testing data group is used for the function test in the neural network.

B. Create a variable set in each layer.

An input variable set in each layer is created. The assembled number is $p!/[(p-r)!r!]$, where p is the number of input variables and r is normally set to be 2.

C. Organization of the neural cell.

To describe the organization of the neural cell with a partial differential characteristic in a nonlinear system, a recursive analysis and data training are utilized step by step. By using AIC (Akaike's information criterion), a domain variable is selected. The output variable of the best neural cell is called the intermediate variable. The best cell is selected from various neural structures in the GMDH neural network.

D. Select the intermediate variable.

The L number of the created intermediate variables with the smallest AIC is selected. To minimize the AIC, a larger L is required.

E. Stopping the internal calculation between layers.

When the decrement error in each layer stops, the internal calculation will terminate. The complete neural network in the non-linear system can be constructed by creating neural cells in each layer.

Polynomial neural network build up

As indicated in Figure 3, the polynomial neural network is composed of an input layer, a hidden layer Σ (Summation), and an output layer (product), where the hidden layer is the weight summation and output layer is the product of the input and weighted value (Patrikar and Provence, 1996). Therefore, the j th output z_{jk} is

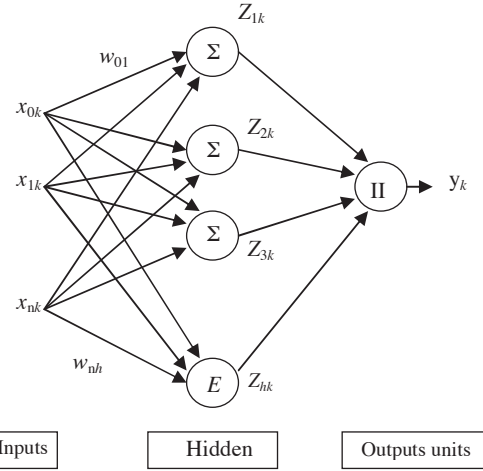


Figure 3. Organization of the polynomial neural network.

$$z_{jk} = \sum_{i=0}^n W_{ij} X_{ij} \tag{9}$$

The total output of the neural network is expressed as

$$y_k = \prod_{j=1}^h z_{jk} \tag{10}$$

where h is the unit's number in a hidden layer.

Combining Eqs. (9) and (10) gives

$$y_k = B_0 + \sum_{i=1}^n B_i x_i + \sum_{i=1}^n \sum_{j=1}^n B_{ij} x_i x_j + \sum_{i=1}^n \sum_{j=1}^n \sum_{k=1}^n B_{ijk} x_i x_j x_k + \dots \tag{11}$$

where y_k is the output value, x_i, x_j, x_k are the input data, and $B_0, B_i, B_{ij},$ and B_{ijk} are the coefficient of the node function.

System training on NNM

To obtain the NNM, using the theoretical data of the TMM as the input data (silencer dimensions such as $D_1, D_2,$ and L_2) and the output data (STL) in the proposed NNM, the trained NNM can be achieved using both the training data bank and the polynomial calculation in conjunction with the PSE standard (deviation of mean square).

PSE is expressed as

$$PSE = FSE + k_p \tag{12}$$

$$FSE = \frac{1}{N} \sum_{i=1}^N (\hat{y}_i - y_i)^2 \tag{13}$$

where FSE is the deviation of mean square, k_p is the penalty function, N is the number of training data, \hat{y}_i is the required data, and y_i is the predicted data for NNM.

The penalty function k_p can be expressed as

$$k_p = \text{CPM} \frac{2\sigma p^2 Q}{N} \quad (14)$$

where CPM is the product of the penalty function; Q is the number of the network's coefficients, and σp^2 is the error variation.

The steps of the NNM construction shown in Figure 4 include the following:

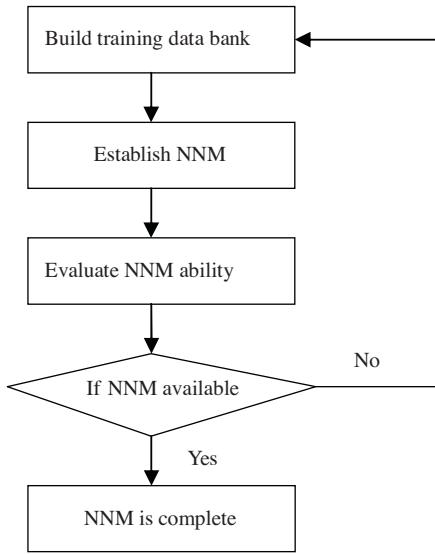


Figure 4. The steps in NNM.

- A. Building up the data bank for network training.

The data bank is used to construct a polynomial neural network. It can be divided into 2 parts, the training data and the testing data one is adopted for the training of the NNM, and the other is for the evaluation purpose of the NNM.

- B. Building up the neural network model.

By selecting the number and type of layer and using the trained data bank in the chosen network, a neural network model can be built.

- C. Evaluate the ability of the NNM.

After the NNM is established, the function test using the testing data is required for evaluating the ability of the NNM.

- D. Usage of the NNM

The predicted STL can be obtained by inputting arbitrary design data. The NNM, an OBJ function, works in conjunction with the GA optimizer during the optimization process.

Model Check

TMM accuracy check

Before performing the GA optimal simulation on mufflers, an accuracy check of the mathematical model on the fundamental element—a single-chamber muffler shown in Figure 5 was performed using experimental data from Kim et al. (1990). As revealed in Figure 5, the accuracy between the TMM and the experimental data for the single-chamber muffler model is roughly in agreement. Thus, the proposed fundamental mathematical model is valid under the theoretical cutoff frequency of $f_c = \frac{\pi c_0}{1.84D} (1 - M_1^2)^{1/2} = 5422(\text{Hz})$ in which D is the maximum diameter and

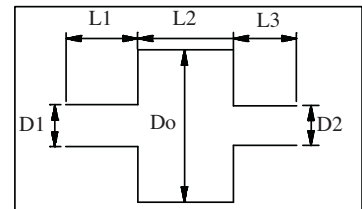
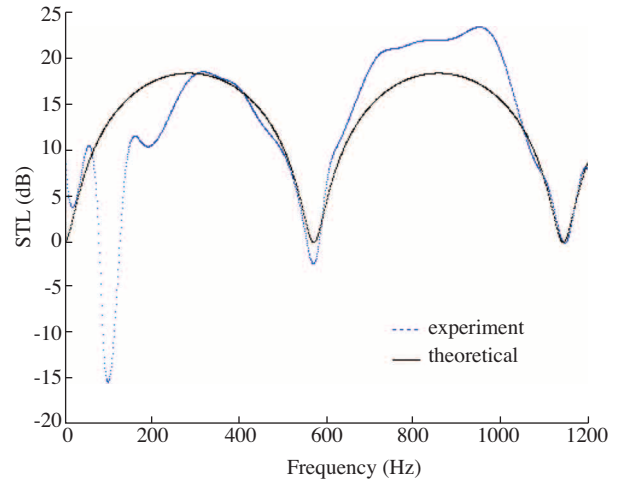


Figure 5. Performance of a single-chamber muffler without the mean flow. [$D_1 = D_2 = 0.0365(\text{m})$, $D_0 = 0.15(\text{m})$, $L_1 = L_3 = 0.1(\text{m})$, $L_2 = 0.3(\text{m})$] [Experiment data are from Kim et al. (1990)].

M_1 is the Mach number. Consequently, the developed model of one-chamber mufflers in conjunction with the NNM and the GA is applied to the shape optimization in the following section.

NNM accuracy check

Before using the NNM as an OBJ function in the GA optimization, an accuracy check of the NNM is performed and shown in Table 1. The result reveals that the accuracy for the target tones (500, 1000, and 2000 Hz) between NNM and TMM is within 91.35~99.78%. This is acceptable.

Genetic Algorithm

The concept of genetic algorithms, first formalized by Holland (1975) and later extended to functional optimization by D. Jong (1975), involves the use of optimization search strategies patterned after the Dar-

winian notion of natural selection. During a GA optimization, one set of trial solutions is chosen and “evolved” toward an optimal solution. For the optimization of the objective function (OBJ), the design parameters are determined.

As the block diagram indicates in Figure 6, the GA accomplishes the task of optimization by starting with a random “population” of values for the parameters of an optimization problem. Subsequently, a new “generation” with an improved objective function value is produced. In order to achieve evolution in a new generation, the binary system, a representation of real numbers and integers, is used. In addition, by manipulating the strings, the operators of reproduction, crossover, mutation, and elitism are worked sequentially.

The operations in the GA method are pictured in Figure 7. The process was terminated when a number of generations exceeded a pre-selected value of $iter_{max}$.

Table 1. Comparison of the STL (at 500 Hz) between the TMM and NNM.

Target tone (Hz)	STL (TMM)	STL (NNM)	deviation (%)
500	23.55301	23.50177	0.2176
1000	23.19912	23.542318	1.48
2000	22.49063	24.43637	8.65

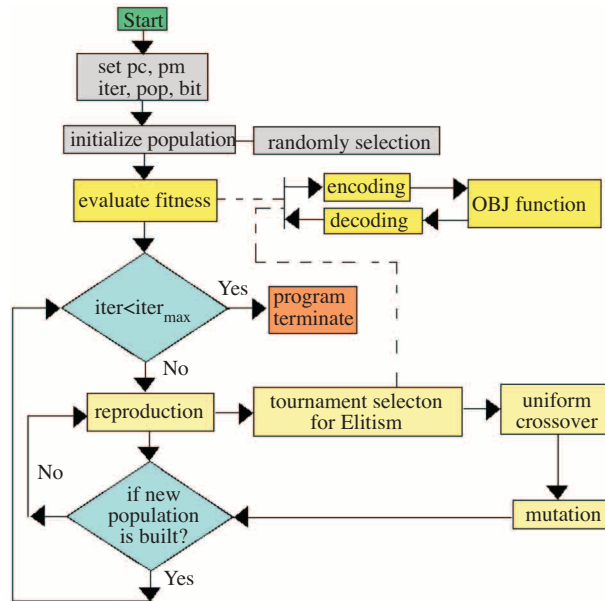


Figure 6. The block diagram of the GA optimization on mufflers.

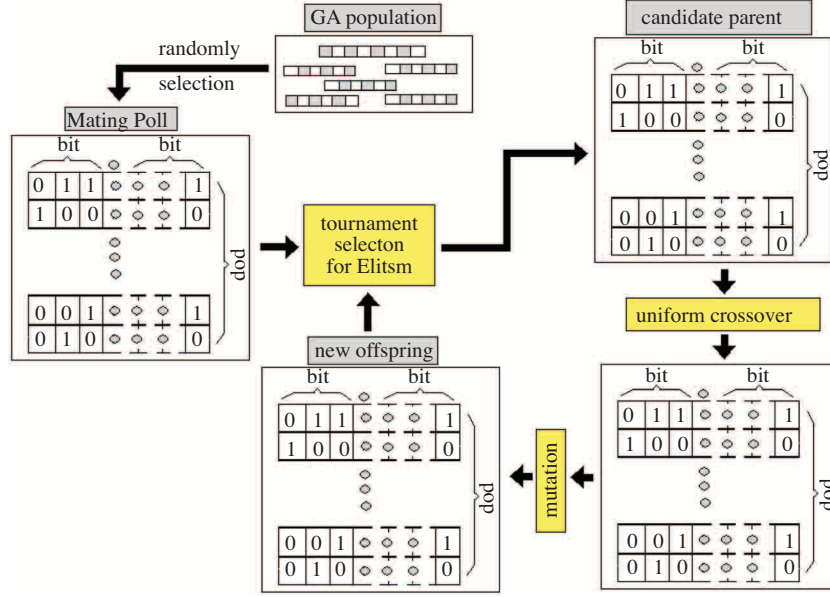


Figure 7. Operations in GA method.

Case Studies

In this paper, an original muffler ($D_1 = D_3 = 0.03654(\text{m})$; $D_2 = 0.108(\text{m})$; $L_1 = L_3 = 0.1(\text{m})$; $L_2 = 0.208(\text{m})$) without shape optimization shown in Figures 1 and 2 is introduced. Under space-constrained condition, the total length of $L_1 + L_2 + L_3$ and the diameter of the expansion chamber D_2 are fixed. To achieve a higher acoustical performance (STL), 3 kinds of design parameters D_1 , D_3 , and L_2 are chosen as the tuned variables. Therefore, the STL in Eq. (8) in the TMM is simplified as

$$STL(D_1, D_3, L_2) = 20 \log \left(\frac{|T_{11}^* + T_{12}^* + T_{21}^* + T_{22}^*|}{2} \right) + 10 \log \left(\frac{S_1}{S_5} \right) \quad (15)$$

Using D_1 , D_3 , and L_2 as the 3 input data and the STL as output data in the NNM and entering a series of training data into the NNM system, the NNM is built as below:

$$N1 = -4.69515 + 22.5728 \times L_2$$

$$N2 = -4.69515 + 43.4736 \times D_2$$

$$N3 = -4.69515 + 128.634 \times D_1$$

$$\begin{aligned} \text{Triple5} = & 0.107327 - 0.224287 \times N1 + 0.673103 \\ & \times N2 - 0.66041 \times N3 - 0.148289 \times N1^2 - 0.0529175 \\ & \times N2^2 + 0.093014 \times N3^2 - 0.0262852 \times N1 \times N2 \\ & + 0.0239928 \times N1 \times N3 - 0.0378132 \times N2 \times N3 - \\ & 0.0117142 \times N1^3 - 0.010688 \times N3^3 \end{aligned}$$

$$U4 = \text{STL} = 11.8005 + 5.19809 \times \text{Triple5}$$

The related NNM diagram is shown in Figure 8. In addition, the searching range of D_1 , D_3 , and L_2 is illustrated in Table 2.

Three kinds of tones (500, 1000, and 2000 Hz) are chosen as the targeted frequencies during the numerical optimization.

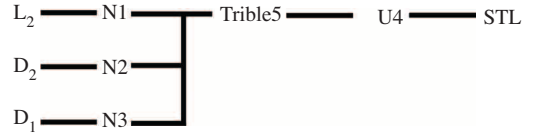


Figure 8. NNM diagram.

Table 2. Constrained condition in a simple expansion muffler.

	Min. (m)	Max. (m)
D_1	0.02555	0.04745
D_3	0.0756	0.1404
L_2	0.1456	0.2704

Results and Discussion

Results

By using the trained NNM in conjunction with the GA optimizer, a series of optimized results are obtained. The best GA set is (pop , bit , $iter_{max}$, pc , pm) = (50, 20, 500, 0.8, 0.05). The resultant optimizations with respect to the targeted tones (500,

Table 3. Comparison of the acoustical performance with and without shape optimization at various frequencies.

Targeted frequency	Optimized muffler				Original muffler
	D_1 (m)	D_3 (m)	L_2 (m)	STL (dB)	STL (dB)
500 Hz	0.0256	0.1397	0.1736	23.46266	12.41989
1000 Hz	0.0256	0.1396	0.2497	23.41351	9.439265
2000 Hz	0.0257	0.1403	0.2127	23.47392	12.82286
Note: for original muffler - $D_1 = 0.03654$; $D_3 = 0.03654$; $L_2 = 0.208$					

1000, and 2000 Hz) are shown in Table 3. Their STL curves, with and without optimization, are plotted in Figures 9, 10, and 11. As indicated in Table 3 it is obvious that the acoustical performance (STL) is improved from 12.4 to 23.4 dB. In addition, the acoustical performance (STL) at the targeted 1000 Hz is improved from 9.4 to 23.4 dB. Moreover, the acoustical performance (STL) at the targeted 2000 Hz is improved from 12.8 to 23.4 dB.

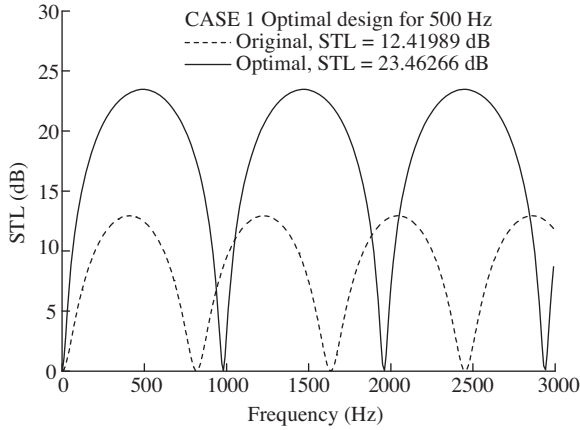


Figure 9. STL with and without optimization (targeted frequency: 500 Hz).

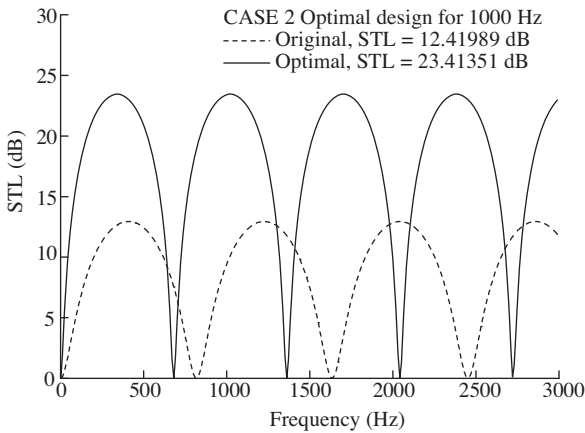


Figure 10. STL with and without optimization (targeted frequency: 1000 Hz).

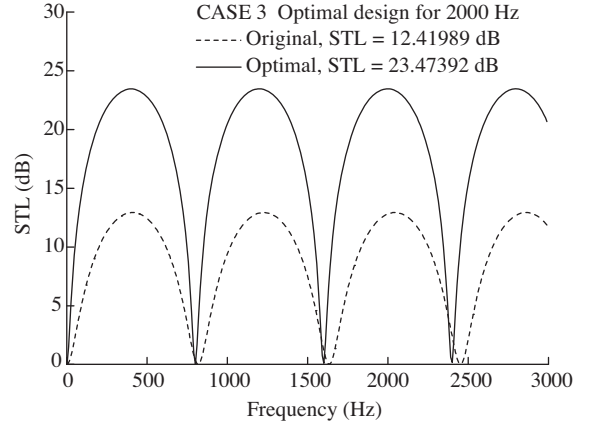


Figure 11. STL with and without optimization (targeted frequency: 2000 Hz).

Discussion

As mentioned above, in the first instance of shape optimization for a targeted frequency at 500 Hz, the sound transmission loss of a muffler at the designed frequency (500 Hz) can be increased by 11 dB after the muffler’s shape optimization. In addition, in the second instance of shape optimization for a targeted frequency at 1000 Hz, the sound transmission loss of a muffler at the designed frequency (1000 Hz) can be increased by 14 dB after the shape optimization is performed. In the third instance of shape optimization for a targeted frequency at 2000 Hz, the sound transmission loss of a muffler can be increased by 10.6 dB after the shape optimization is carried out. The numerical result also indicated that the optimal STL occurred at the smallest and the largest D_2 . Moreover, as indicated in Figures 9-11, the optimized STLs are precisely located at the targeted frequencies of 500, 1000, and 2000 Hz.

Conclusion

The present paper has shown that the perforated muffler can be precisely optimized at a targeted

frequency using the NNM in concert with the GA method by adjusting the muffler's shape under space constraints.

To simplify the calculation in the OBJ function during GA optimization, a trained neural network model (NNM) is established and used as a new OBJ function. Before optimization is performed, the accuracy of the theoretical mathematical model (TMM) is checked and confirmed by the experimental data. Moreover, the TMM's STL and the NNM's STL are similar. Furthermore, the optimal values of the STL achieved at the target frequencies reveal that the NNM along with the GA optimizer in the one-chamber mufflers was applicable. Therefore, from an economic point of view, the GA approach becomes effective because of its speed and because there is no need for either a starting point or a mathematical derivation in the traditional gradient method. Finally, the use of the GA optimization as well as the NNM in the one-chamber mufflers' shape design is more efficient when compared to the trial calculations and tests conducted in the laboratory.

Acknowledgements

The authors acknowledge the financial support of Tatung University (B95-M06-049) and the National Science Council (NSC 95-2218-E-235-002).

Nomenclature

C_o	sound speed (m s^{-1})
D_1, D_3	diameter of the inlet/outlet duct (m)
D_2	diameter of the expansion chamber (m)
f	frequency (Hz)
f_c	cutoff frequency (Hz)
j	imaginary unit
$iter_{\max}$	maximum iteration
k	wave number ($=\frac{\omega}{c_o}$)
L_1, L_3	lengths of inlet/outlet ducts (m)
L_2	length of the expansion chamber (m)
M	mean flow Mach number in the straight duct
OBJ	objective function
pc	crossover ratio
p_i	acoustic pressure at i th node (Pa)
pm	mutation ratio
pop	no. of population
Q	volume flow rate of venting gas ($\text{m}^3 \text{s}^{-1}$)
S_i	section area at i th element (m^2)
STL	sound transmission loss (dB)
TS_{ij}	components of a 4-pole transfer matrix for a straight duct
TE_{ij}	components of a 4-pole transfer matrix for an expanded and contracted duct
T_{ij}	components of a 4-pole transfer system matrix
u_i	acoustic particle velocity at i th node (m s^{-1})
ρ_o	air density (kg m^{-3})

References

- Alley, B.C., Dufresne, R.M., Kanji, N. and Reesal, M.R., "Costs of Workers' Compensation Claims for Hearing Loss", *Journal of Occupational Medicine*, 31, 134-138, 1989.
- Chang, Y.C., Yeh, L.J. and Chiu, M.C., "Shape Optimization on Constrained Single-chamber Muffler by Using GA Method and Mathematical Gradient Method", *International Journal of Acoustics and Vibration*, 10, 17-25, 2005.
- Chang, Y.C., Yeh, L.J., Chiu, M.C. and Lan, T.S., "Shape Optimal Design on Constrained Single-Chamber Mufflers by Gradient Method", *De Lin Journal*, 18, 41-54, 2004.
- Davis, D.D., Stokes, J.M. and Moorse, L., "Theoretical and Experimental Investigation of Mufflers with Components on Engine Muffler Design", NACA Report, 1192, 1954.
- Holland, J.H., "Adaptation in Natural and Artificial System", Ann Arbor, MI, The University of Michigan Press, 1975.
- Igarashi, J. and Arai, M., "Fundamentals of Acoustical Silencers, Part 3: Attenuation Characteristic Studies by Electric Simulator", Report, Aeronaut Res. Inst. University of Tokyo, 351, 17-31, 1960.
- Igarashi, J. and Toyama, M., "Fundamentals of Acoustical Silencers, Part 1: Theory and Experiment of Acoustic Low-pass Filters", Report, Aeronaut Res. Inst. University of Tokyo, 339, 223-241, 1958.
- Ivakhnenko, A.G., "Polynomial Theory of Complex System", *IEEE Trans. Syst. Man. Cyber.*, 1, 364-368, 1971.
- Jong, D., "Analysis of the Behavior of a Class of Genetic Adaptive Systems", PhD Dissertation, The University of Michigan Press, 1975.

Kaiser, L. and Bernhardt, H., "Noise Control on Computer and Business Equipment Using Speed Control Blowers", IEEE, 2, 114-117, 1989.

Kim, Y.H., Choi, J.W. and Lim, B.D., "Acoustic Characteristics of an Expansion Chamber with Constant Mass Flow and Steady Temperature Gradient (Theory and Numerical Simulation)", Journal of Vibration and Acoustics, 112, 460-467, 1990.

Kondo, T., "The Learning Algorithms of the GMDH Neural Network and Their Application to Medical Image Recognition", SICE, 1988.

Magrab, E.B., "Environmental Noise Control; John Wiley & Sons, New York, 1975.

Miwa, T. and Igarashi, J., Fundamentals of Acoustical Silencers, Part 2: Determination of Four Terminal Constants of Acoustical Element", Report, Aeronaut Res. Inst. University of Tokyo, 344, 67-85, 1959.

Munjal, M.L., "Acoustics of Ducts and Mufflers with Application to Exhaust and Ventilation System Design", John Wiley & Sons, New York, 1987.

Patrikar, A. and Provence, J., "Nonlinear System Identification and Adaptive Control Using Polynomial Networks", Math. Comput. Modeling, 123, 159-173, 1996.

Prasad, M.G., "A Note on Acoustic Plane Waves in a Uniform Pipe with Mean Flow", Journal of Sound and Vibration, 95, 284-290, 1984.